Springer

KSME

Journal of Mechanical Science and Technology 26 (8) (2012) 2459~2467
www.springerlink.com/content/1738-494x
DOI 10.1007/s12206-012-0628-8

Semi-active vibration control of an eleven degrees of freedom suspension system using neuro inverse model of magnetorheological dampers †

Seiyed Hamid Zareh[1,*], Meisam Abbasi[1], Hadi Mahdavi[2] and Kambiz Ghaemi Osgouie[1]

[1]*School of Science and Engineering, Sharif University of Technology, Iran*
[2]*Department of Mechanical Engineering, Shahid Bahonar University of Kerman, Kerman, Iran*

(Manuscript Received September 22, 2011; Revised March 8, 2012; Accepted March 26, 2012)

Abstract

A semi-active controller-based neural network for a suspension system with magnetorheological (MR) dampers is presented and evaluated. An inverse neural network model (NIMR) is constructed to replicate the inverse dynamics of the MR damper. The typical control strategies are linear quadratic regulator (LQR) and linear quadratic gaussian (LQG) controllers with a clipped optimal control algorithm, while inherent time-delay and non-linear properties of MR damper lie in these strategies. LQR part of LQG controller is also designed to produce the optimal control force. The LQG controller and the NIMR models are linked to control the system. The effectiveness of the NIMR is illustrated and verified using simulated responses of a full-car model. The results demonstrate that by using the NIMR model, the MR damper force can be commanded to follow closely the desirable optimal control force. The results also show that the control system is effective and achieves better performance and less control effort than the optimal in improving the service life of the suspension system and the ride comfort of a car.

Keywords: Clipped optimal algorithm; Inverse model; MR damper; Neural network; Semi-active control; Suspension system

1. Introduction

Suspension systems have long been of great concern for car manufacturing industries. They perform multiple tasks such as maintaining contact between vehicle tires and the road, addressing the stability of the vehicle, and isolating the frame of the vehicle from road-induced vibration and shocks. In general, ride comfort, road handling, and stability are the most important factors in evaluating suspension performance.

In the present study, the suspension system of a passenger car is modified to reduce the amplitude of the car vibration caused by applied road profile. In the passive suspension system, the stiffness and damping parameters are fixed and effective over a certain range of frequencies.

To overcome this problem, the use of semi-active suspension systems which have the capability of adapting themselves to changing road conditions by using an actuator has been considered; therefore an MR damper is added to an ordinary suspension system while the other parts of the suspension system are intact. The significance of the MR damper is that its viscosity changes as the magnetic field changes. A schematic model of the MR damper is shown in Fig. 1.

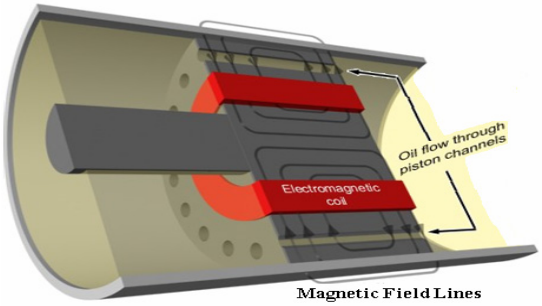

Fig. 1. Schematic model of MR damper.

The considered suspension model is controlled by the applied LQR and LQG controllers. By using employed controller results, the amount of viscosity of the MR damper incorporated with the clipped optimal strategy can be calculated. Unfortunately, due to the inherent nonlinear nature of the MR damper to generate force, a model like that for its inverse dynamics is difficult to mathematically obtain. For this reason, an inverse neural network model is constructed to copy the inverse dynamics of the MR damper.

Interest in a new class of computational intelligence systems known as Artificial Neural Networks (ANNs) has grown in the last few years. This type of network has been found to be a powerful computational tool for organizing and correlating

*Corresponding author. Tel.: +989378550656, Fax.: +987224223895
E-mail address: zareh_hamid@alum.sharif.edu
† Recommended by Associate Editor Hyoun Jin Kim

information in ways that have been proven to be useful for solving certain types of complex and poorly understood problems. The applications of ANNs to the area of structural control have rapidly grown through system identification, system inverse identification or controller replication.

The intelligent neuro-fuzzy and fuzzy inverse model strategies for semi-active suspension system are utilized by Zareh et al. [1, 2]. Narayanan et al. [3] applied a half car model for simulating the semi-active suspension system. They modeled MR damper parameters by the modified Bouc–Wen model and determined that they fit the hysteretic behavior. Vibration control of a passenger car utilizing a half car model was discussed by Yahaya et al. [4]. To improve the accuracy of car model Zareh et al. [5], modeled the vehicle suspension system using a full car model in which the accuracy of the model improved components to quarter-car and half-car models.

Semi-active and active control methods have been developed using different actuators such as Electro-Rheological (ER) and MR dampers. Salem et al. [6] controlled an active quarter-car suspension system by fuzzy logic controller. Sohn et al. [7] utilized an adaptive LQG controller for semi-active suspension systems for a quarter-car model. Golnaraghi et al. [8] controlled a semi-active quarter car suspension system intelligently. They utilized an inverse mapping model to estimate the current based on an artificial neural network and incorporated it into the fuzzy logic controller.

The previous studies made full use of the advantages of the neural network and the optimal controllers and solved the different problems which lay in the suspension system. Few studies included the combination of the two techniques (LQG and neural network in that it is more applicable) to solve the time-delay and the inherent nonlinear nature of the MR damper to generate force instantaneously choosing control parameters in semi-active control or active control for full car models with high degrees of freedom. In this paper, four MR dampers are added to a suspension system between body and wheels in parallel with the passive dampers.

For the intelligent system, a three-layer feed forward neural network, trained on-line under the Levenberg–Marquardt (LM) algorithm, is adopted. In order to verify the effectiveness of the proposed NIMR control strategy, the uncontrolled system and the clipped optimal controlled suspension system are compared with the NIMR controlled system. Through a numerical example under actual road profile excitation, it can be concluded that the control strategy is very important for semi-active control, that the NIMR control strategy can determine currents of the MR damper quickly and accurately, and that the control effect of the NIMR control strategy is better than the others.

2. Full car model

In the full-car model, 11-DOFs are assumed, and all wheels and passengers are dependent on each other and on the car body. It is assumed that each wheel has an effect on the spring and the damper of other wheels, and the two axes of the vehicle are relevant. The MR actuator is utilized to damp the effect of road profile on the passengers. Note that the MR shock absorber is added to the axel and the car body. In the full-car model, the effect of body rotations around roll and the yaw axis is simulated. The suspension system using the full-car model has 11-DOFs, four of which for the four wheels, three for the body displacement and its rotations and the last four for passengers. The schematic of the full-car model with 11-DOFs and an additional MR damper is shown in Fig. 2.

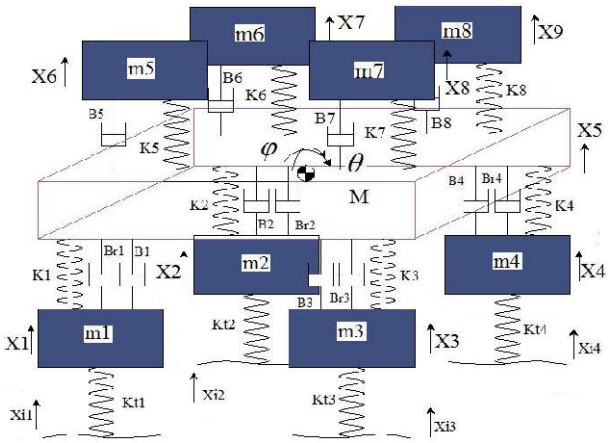

Fig. 2. Full-car model with 11-DOFs [1].

The state space form and the corresponding matrices are observed in Eqs. (1)-(7) [1]. **E** is the location matrix of the actuators. Matrices **K**, **S** and **T** are defined as stiffness, damping coefficient and input matrix due to the wheels stiffness, respectively.

In Eq. (1) x, u and w are states of system, control signal from actuators and input road profile respectively.

$$\dot{x} = Ax + Bu + Gw \tag{1}$$

$$A = \begin{bmatrix} 0 & I \\ -M^{-1}K & -M^{-1}S \end{bmatrix} \tag{2}$$

$$B = \begin{bmatrix} 0 \\ M^{-1}T \end{bmatrix} \tag{3}$$

$$G = \begin{bmatrix} 0 \\ M^{-1}E \end{bmatrix} \tag{4}$$

$$M = diag(m_1, m_2, m_3, m_4, M_b, m_5, m_6, m_7, m_8, I_1, I_2) \tag{5}$$

$$T = [k_{t1},0,0,0;\ 0,k_{t2},0,0;\ 0,0,\ k_{t3},0;\ 0,0,0,k_{t4};\ zeros(7,4)] \tag{6}$$

$$E = [-eye(4,4);1,1,1,1;\ zeros(4,4);\ r_{11},r_{21},\ -r_{31},-r_{41};r_{12},-r_{22},r_{32},-r_{42}] \tag{7}$$

$$K = \begin{bmatrix}
+k_1+k_{t1} & 0 & 0 & 0 & -k_1 & 0 & 0 & 0 & 0 & -k_1r_{11} & -k_1r_{12} \\
0 & +k_2+k_{t2} & 0 & 0 & -k_2 & 0 & 0 & 0 & 0 & -k_2r_{21} & +k_2r_{22} \\
0 & 0 & +k_3+k_{t3} & 0 & -k_3 & 0 & 0 & 0 & 0 & +k_3r_{31} & -k_3r_{32} \\
0 & 0 & 0 & +k_4+k_{t4} & -k_4 & 0 & 0 & 0 & 0 & +k_4r_{41} & +k_4r_{42} \\
-k_1 & -k_2 & -k_3 & -k_4 & \begin{matrix}+k_1+k_2+k_3+k_4\\+k_5+k_6+k_7+k_8\end{matrix} & -k_5 & -k_6 & -k_7 & -k_8 & \begin{matrix}+k_1r_{11}+k_2r_{21}-k_3r_{31}\\-k_4r_{41}+k_5r_{51}\\+k_6r_{61}-k_7r_{71}-k_8r_{81}\end{matrix} & \begin{matrix}+k_1r_{12}-k_2r_{22}+k_3r_{32}\\-k_4r_{42}+k_5r_{52}\\-k_6r_{62}+k_7r_{72}-k_8r_{82}\end{matrix} \\
0 & 0 & 0 & 0 & -k_5 & +k_5 & 0 & 0 & 0 & -k_5r_{51} & -k_5r_{52} \\
0 & 0 & 0 & 0 & -k_6 & 0 & +k_6 & 0 & 0 & -k_6r_{61} & +k_6r_{62} \\
0 & 0 & 0 & 0 & -k_7 & 0 & 0 & +k_7 & 0 & +k_7r_{71} & -k_7r_{72} \\
0 & 0 & 0 & 0 & -k_8 & 0 & 0 & 0 & +k_8 & +k_8r_{81} & +k_8r_{82} \\
-k_1r_{11} & -k_2r_{21} & +k_3r_{31} & +k_4r_{41} & \begin{matrix}+k_1r_{11}+k_2r_{21}-k_3r_{31}\\-k_4r_{41}+k_5r_{51}\\+k_6r_{61}-k_7r_{71}-k_8r_{81}\end{matrix} & -k_5r_{51} & -k_6r_{61} & +k_7r_{71} & +k_8r_{81} & \begin{matrix}+k_1r_{11}^2+k_2r_{21}^2+k_3r_{31}^2\\+k_4r_{41}^2+k_5r_{51}^2\\+k_6r_{61}^2+k_7r_{71}^2+k_8r_{81}^2\end{matrix} & \begin{matrix}+k_1r_{11}r_{12}-k_2r_{21}r_{22}-k_3r_{31}r_{32}\\+k_4r_{41}r_{42}+k_5r_{51}r_{52}\\-k_6r_{61}r_{62}-k_7r_{71}r_{72}+k_8r_{81}r_{82}\end{matrix} \\
-k_1r_{12} & +k_2r_{22} & -k_3r_{32} & +k_4r_{42} & \begin{matrix}+k_1r_{12}-k_2r_{22}+k_3r_{32}\\-k_4r_{42}+k_5r_{52}\\-k_6r_{62}+k_7r_{72}-k_8r_{82}\end{matrix} & -k_5r_{52} & +k_6r_{62} & -k_7r_{72} & +k_8r_{82} & \begin{matrix}+k_1r_{11}r_{12}-k_2r_{21}r_{22}-k_3r_{31}r_{32}\\+k_4r_{41}r_{42}+k_5r_{51}r_{52}\\-k_6r_{61}r_{62}-k_7r_{71}r_{72}+k_8r_{81}r_{82}\end{matrix} & \begin{matrix}+k_1r_{12}^2+k_2r_{22}^2+k_3r_{32}^2+k_4r_{42}^2\\+k_5r_{52}^2\\+k_6r_{62}^2+k_7r_{72}^2+k_8r_{82}^2\end{matrix}
\end{bmatrix} \quad (8)$$

$$S = \begin{bmatrix}
+B_1 & 0 & 0 & 0 & -B_1 & 0 & 0 & 0 & 0 & -B_1r_{11} & -B_1r_{12} \\
0 & +B_2 & 0 & 0 & -B_2 & 0 & 0 & 0 & 0 & -B_2r_{21} & +B_2r_{22} \\
0 & 0 & +B_3 & 0 & -B_3 & 0 & 0 & 0 & 0 & +B_3r_{31} & -B_3r_{32} \\
0 & 0 & 0 & +B_4 & -B_4 & 0 & 0 & 0 & 0 & +B_4r_{41} & +B_4r_{42} \\
-B_1 & -B_2 & -B_3 & -B_4 & \begin{matrix}+B_1+B_2+B_3+B_4\\+B_5+B_6+B_7+B_8\end{matrix} & -B_5 & -B_6 & -B_7 & -B_8 & \begin{matrix}+B_1r_{11}+B_2r_{21}-B_3r_{31}\\-B_4r_{41}+B_5r_{51}\\+B_6r_{61}-B_7r_{71}-B_8r_{81}\end{matrix} & \begin{matrix}+B_1r_{12}-B_2r_{22}+B_3r_{32}\\-B_4r_{42}+B_5r_{52}\\-B_6r_{62}+B_7r_{72}-B_8r_{82}\end{matrix} \\
0 & 0 & 0 & 0 & -B_5 & +B_5 & 0 & 0 & 0 & -B_5r_{51} & -B_5r_{52} \\
0 & 0 & 0 & 0 & -B_6 & 0 & +B_6 & 0 & 0 & -B_6r_{61} & +B_6r_{62} \\
0 & 0 & 0 & 0 & -B_7 & 0 & 0 & +B_7 & 0 & +B_7r_{71} & -B_7r_{72} \\
0 & 0 & 0 & 0 & -B_8 & 0 & 0 & 0 & +B_8 & +B_8r_{81} & +B_8r_{82} \\
-B_1r_{11} & -B_2r_{21} & +B_3r_{31} & +B_4r_{41} & \begin{matrix}+B_1r_{11}+B_2r_{21}-B_3r_{31}\\-B_4r_{41}+B_5r_{51}\\+B_6r_{61}-B_7r_{71}-B_8r_{81}\end{matrix} & -B_5r_{51} & -B_6r_{61} & +B_7r_{71} & +B_8r_{81} & \begin{matrix}+B_1r_{11}^2+B_2r_{21}^2+B_3r_{31}^2\\+B_4r_{41}^2+B_5r_{51}^2\\+B_6r_{61}^2+B_7r_{71}^2+B_8r_{81}^2\end{matrix} & \begin{matrix}+B_1r_{11}r_{12}-B_2r_{21}r_{22}-B_3r_{31}r_{32}\\+B_4r_{41}r_{42}+B_5r_{51}r_{52}\\-B_6r_{61}r_{62}-B_7r_{71}r_{72}+B_8r_{81}r_{82}\end{matrix} \\
-B_1r_{12} & +B_2r_{22} & -B_3r_{32} & +B_4r_{42} & \begin{matrix}+B_1r_{12}-B_2r_{22}+B_3r_{32}\\-B_4r_{42}+B_5r_{52}\\-B_6r_{62}+B_7r_{72}-B_8r_{82}\end{matrix} & -B_5r_{52} & +B_6r_{62} & -B_7r_{72} & +B_8r_{82} & \begin{matrix}+B_1r_{11}r_{12}-B_2r_{21}r_{22}-B_3r_{31}r_{32}\\+B_4r_{41}r_{42}+B_5r_{51}r_{52}\\-B_6r_{61}r_{62}-B_7r_{71}r_{72}+B_8r_{81}r_{82}\end{matrix} & \begin{matrix}+B_1r_{12}^2+B_2r_{22}^2+B_3r_{32}^2+B_4r_{42}^2\\+B_5r_{52}^2\\+B_6r_{62}^2+B_7r_{72}^2+B_8r_{82}^2\end{matrix}
\end{bmatrix} \quad (9)$$

where M_b, m_1, m_2, m_3, m_4, m_5, m_6, m_7 and m_8 stand for the mass of the car body, masses of the four wheels and mass of passengers, respectively. I_1 and I_2 are the moments of inertia of the car body around the two axes, respectively.

The terms k_1, k_2, k_3, k_4, k_5, k_6, k_7 and k_8 are the stiffness of the springs of the suspension system and the stiffness of the springs of the passenger seat, respectively. The terms k_{t1}, k_{t2}, k_{t3} and k_{t4} are the stiffness of the tires. The terms b_1, b_2, b_3, b_4, b_5, b_6, b_7 and b_8 are the coefficients of the car and the passenger seat dampers, respectively.

Then, b_{r1}, b_{r2}, b_{r3} and b_{r4} are the coefficients of the MR dampers, respectively. x_1, x_2, x_3, x_4, x_5, x_6, x_7, x_8, x_9, φ and θ indicate the DOFs of the suspension system model, respectively. The terms x_{i1}, x_{i2}, x_{i3} and x_{i4} indicate the load profile disturbance, respectively.

The numerical values of the model dimensions for obtaining the responses are shown in Table 1 [1].

3. NIMR control strategy

Fig. 3 illustrates the proposed NIMR control strategy. There is basically no restriction on the type of control algorithm that should be used as long as it calculates a desirable control force f_c based on the response and/or excitation. The desirable control force and the response of the systems are passed in to the inverse NN model. This NN model emulates inverse dynamics of the MR damper. The output of this inverse NN model is the voltage required to produce the desire control force under the current response condition. This voltage is an/the input to the MR damper which then produces force f acting on the

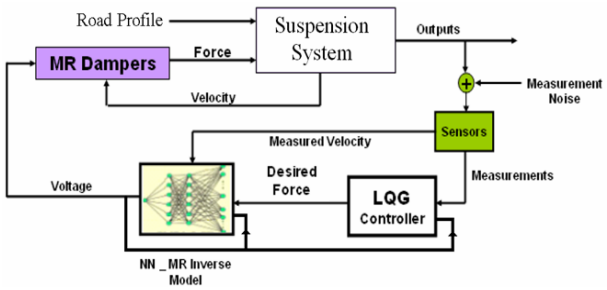

Fig. 3. NIMR control strategy block diagram.

Table 1. Numerical values of model.

Symbol	Quantity	Value
M_b	Mass of car body (kg)	670
I_1	Inertia around yaw (kg/m^2)	800
I_2	Inertia around roll (kg/m^2)	1100
$m_{1\text{-}4}$	Mass of wheels (kg)	30
$m_{5\text{-}8}$	Mass of passengers (kg)	120
$k_{1\text{-}4}$	Stiffness of car springs (N/m)	17500
$k_{5\text{-}8}$	Stiffness of seats (N/m)	1750
$b_{1\text{-}4}$	Viscosity of car dampers (Ns/m)	1460
$b_{5\text{-}8}$	Viscosity of seat damper (Ns/m)	700
$k_{t1\text{-}4}$	Stiffness of wheels (N/m)	175500
r_{11}	Length distance between the front left wheel and the mass center (m)	1.9975
r_{12}	Width distance between the front left wheel and the mass center (m)	0.8025
r_{21}	Length distance between the front right wheel and the mass center (m)	1.9975
r_{22}	Width distance between the front right wheel and the mass center (m)	0.8025
r_{31}	Length distance between the back right wheel and the mass center (m)	1.9975
r_{32}	Width distance between the back right wheel and the mass center (m)	0.8025
r_{41}	Length distance between the back left wheel and the mass center (m)	1.9975
r_{42}	Width distance between the back left wheel and the mass center (m)	0.8025
r_{51}	Length distance between the driver seat and the mass center (m)	1.9975
r_{52}	Width distance between the driver seat and the mass center (m)	0.8025
r_{61}	Length distance between the front right seat and the mass center (m)	1.9975
r_{62}	Width distance between the front right seat and the mass center (m)	0.8025
r_{71}	Length distance between the back left seat and the mass center (m)	1.9975
r_{72}	Width distance between the back left seat and the mass center (m)	0.8025
r_{81}	Length distance between the back right seat and the mass center (m)	1.9975
r_{82}	Width distance between the back right seat and the mass center (m)	0.8025

suspension system. Note that, the NN part of control strategy will be trained by the results of clipped optimal strategy.

4. Clipped optimal algorithm

The clipped optimal control strategy for an MR damper usually involves two steps. The first step is to assume an ideal actively–controlled device and construct an optimal controller for this active device. In the second step, a secondary controller finally determines the input voltage of the MR damper [19]. That is, the secondary controller clips the optimal force in a manner consistent with the dissipative nature of the device.

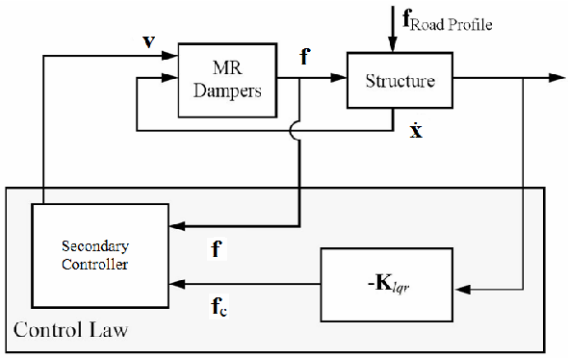

Fig. 4. Clipped optimal algorithm block diagram.

The block diagram of the clipped optimal algorithm is shown in Fig. 4.

The clipped optimal control approach is to append a force feedback loop to induce the MR damper to produce approximately a desired control force f_c. It is known as a control signal (u). The Linear Quadratic Regulator (LQR) algorithm has been employed both for active control and for semi-active control. Using this algorithm, the optimal control force f_c for f, which is force generated by an MR damper, may be obtained by minimizing the following scalar performance index:

$$J = \int_{t_0}^{t_f} (x^T Q x + F^T R F) dt \tag{10}$$

where **Q** and **R** are weighting matrices and their values are selected based on the relative importance given to different terms in their contributions to the performance index **J**.

Solving the optimal control problem with **J** defined by Eq. (10) results in an optimal force vector f_c regulated only by the state vector x, such that:

$$f_C = -(R^{-1} B^T P) x = -K_{lqr} x \tag{11}$$

where matrix K_{lqr} represents the gain matrix; and the matrix **P** is the solution of the Riccati equation given by Eq. (12).

$$PA + A^T P - PBR^{-1} B^T P + Q = 0 \tag{12}$$

Here, Q_{22*22} is an identity matrix (I_{22*22}) because all states are important and the best responses are obtained by this value. R_{4*4} is $45*I_{4*4}$, which is obtained by trial and error to receive the desired response.

The force generated by the MR damper cannot be commanded. When the MR damper is providing the desired optimal force (*i.e.*, $f = f_c$), the voltage applied to the damper should remain at the present level. If the magnitude of the force produced by the damper is smaller than the magnitude of the desired optimal force and the two forces have the same sign, the voltage applied to the current driver [9] varies con-

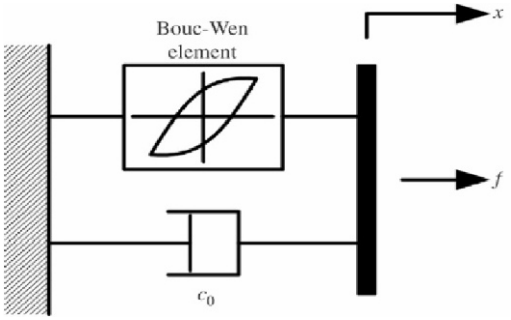

Fig. 5. Mechanical model of a shear mode type MR damper [1].

tinuously in the range of [*0-V_{max}*]. The secondary controller for continuously varying the command voltage can be stated as:

$$v_i = V_{ci} H(\{f_{ci} - f_i\} f_i) \tag{13}$$

$$V_{ci} = \begin{cases} \mu_i f_{ci} & , \quad for \quad f_{ci} \le f_{\max} \\ V_{\max} & , \quad for \quad f_{ci} > f_{\max} \end{cases} \tag{14}$$

where V_{max} is *12v* and f_{max} is the maximum force produced by the damper (*=3,000 N*); μ is the coefficient relating the voltage to the force (*=V_{max}/f_{max}*); *H (.)* is the heaviside step function expressed as 0 or 1 [9]; and f_i is the force produced by i^{th} MR dampers and applied to the structure.

In this paper, a simple mechanical model consisting of a Bouc-Wen element shown in Fig. 5 in parallel with a viscous damper is used. This model has been verified to accurately predict the behavior of a prototype shear-mode MR damper over a wide range of inputs in a set of experiments and is also expected to be appropriate for modeling a full-scale MR damper.

The equations governing the force f_i exerted by this model are as follows:

$$f_i = c_0 \dot{x} + \alpha z \tag{15}$$

$$\dot{z} = -\gamma |\dot{x}| z |\dot{z}|^{n-1} - \beta \dot{x} |z|^n + A_m \dot{x} \tag{16}$$

where x is the displacement of the device, and z is the evolutionary variable that accounts for the history dependence of the response. The parameters γ, β, n and A_m are adjusted to determine the linearity in the unloading and the smoothness of the transition from the pre-yield region to the post-yield region. The device model parameters α and c_0 are determined by the dependency on the control voltage u as follows:

$$\alpha = \alpha(u) = \alpha_a + \alpha_b u \tag{17}$$

$$c_0 = c_0(u) = c_{0a} + c_{0b} u \,. \tag{18}$$

Moreover, to account for a time-lag in the response of the device to the changes in the command input, the first-order filter dynamics are introduced into the system as follows:

Table 2. Numerical values of MR damper model.

α_a (N cm^{-1})	α_b (N cm^{-1} V^{-1})	γ (cm^{-2})	β (cm^{-2})
140	695	363	363

Table 3. Numerical values of MR damper model.

c_{0a} (Nscm^{-1})	c_{0b} (Nscm^{-1} V^{-1})	n	η (s^{-1})	A_m
21	3.5	1	190	301

Table 4. Typical properties of unpaved road profile.

σ^2 (m^2)	ω (rad/s)	V (m/s)	α_r (rad/m)
3e-4	200π	16.66	0.45

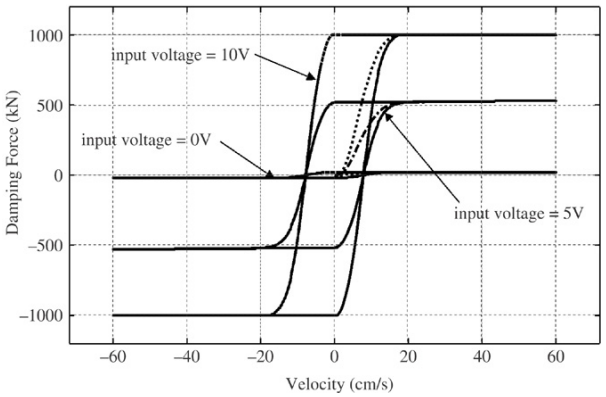

Fig. 6. Hysteretic behavior of an MR damper [1].

$$\dot{u} = -\eta(u - \upsilon) \tag{19}$$

where v is a command voltage applied to the control circuit, and η is the time constant of the first-order filter.

The numerical values of the parameters are shown in Tables 2 and 3 [10].

The hysteretic behavior of the MR damper model according to the input voltage is shown in Fig. 6.

5. Road profile simulation

The random road excitation is generated using white noise as a road irregularity as a disturbance. The Power Spectral Density (PSD) function of the road irregularity is assumed to be in the form of Eq. (20).

$$S_h = \frac{\sigma^2}{\pi} \frac{\alpha_r V}{(\omega^2 + (\alpha_r V)^2)} \tag{20}$$

where σ^2 is the variance of the road profile, ω is the excitation frequency of the road input V is the vehicle forward constant velocity and α_r is a coefficient depending on the type of road surface. The typical properties of the unpaved road profile are shown in Table 4 [3]. The PSD of the road surface is obtained

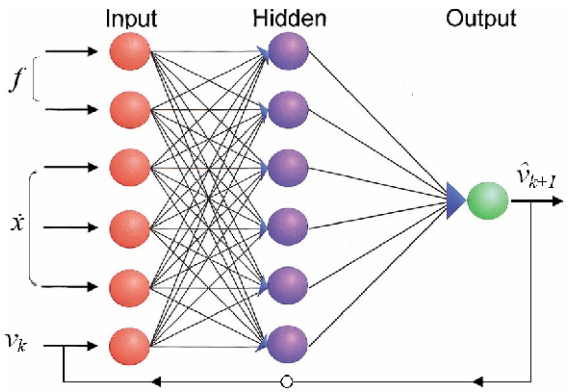

Fig. 7. NN of inverse dynamics of MR damper (NIMR).

using MATLAB®.

6. Neural network inverse dynamics of MR damper

The MR damper model discussed earlier in this paper estimates damper forces based on the inputs of the reactive velocity and the issued voltage as described by Eqs. (15)-(19). Thus, the voltage signal is the only parameter that can be modified to control the damper force to produce the required control force. The control algorithm, LQG, estimates the required optimal control force but the MR damper force is controlled by voltage. In this case, it is essential to develop an inverse dynamic model that predicts the corresponding control voltage to be sent to the damper so that an appropriate damper force can be generated. Unfortunately, due to the inherent nonlinear nature of the MR damper, a model like that for its inverse dynamics is difficult to mathematically obtain. For this reason, a feed-forward back-propagation neural network that is shown in Fig. 7 is constructed to copy the inverse dynamics of the MR damper. The purpose in a vehicle suspension system is reduction of transmittance of vibrational effects from the road to the vehicle's passengers, hence providing ride comfort. To accomplish this, one can first design a clipped algorithm for the suspension system, using an optimal control method and use it to train a neuro controller. Consider network can be trained using the clipped controller output error on an online manner (clipped output selected as a desire targets for training). Once trained, the clipped controller is automatically removed from the control loop and the neuro controller takes on. In case of a change in the parameters of the system under control, the clipped optimal controller enters the control loop again and the neural network gets trained again for the new excitation [16]. An important characteristic of the proposed controller is that no mathematical model is needed for the system components, such as the non-linear actuator or shock absorbers. At the initial time, the inputs of the network will be taken to have the value of zero in accordance with the actual initial circumstance and simplicity in simulation [1, 19, 21]. Before online training, the network trained off-line to achieve

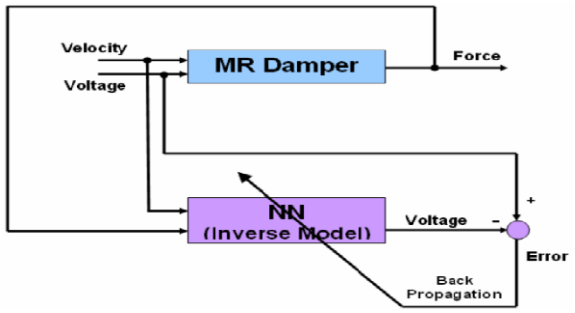

Fig. 8. Training of NIMR.

update weights near to desired.

This model is denoted as NIMR. This neural network model is trained using input-output data generated analytically by using the simulated MR model based on Eqs. (15)-(19). This NIMR calculates the voltage signal as an output based on the current and a few previous histories of measured velocity and desirable control force as inputs. Then the voltage signals are sent to the MR damper so that it can generate the desirable optimal control forces.

Training the NIMR requires the compilation of input-output data. To completely identify the underlying MR system model, the data must contain information about the entire operating range of the system. The generated forces are the results of the MR model described in Eqs. (15)-(19). The sampling data for 10-second periods results in 10000 patterns for training, testing and validation, Fig. 8.

The next step is to select the network architecture. To do so it is required to determine the number of inputs, outputs, hidden layers, and nodes in the hidden layers, and this is usually done by trial and error. The most suitable input data for our case was found to be the current and the three and two previous histories for the velocity ($\dot{x}_{k+2}, \dot{x}_{k+1}, \dot{x}_k$) and the force ($f_{k+1}$, f_k), respectively. Also one hidden layer, which it has six nodes, were adopted as one of the best suitable topologies for the NIMR as can be seen in Fig. 7. This structure obtained by trial and error, because it required minimum time for online training with acceptable accuracy.

The logsigmoid (ranging from 0 to 1) activation function is used for the hidden layer's nodes and the linear function for the output layer's nodes which represents the voltage. 10000 patterns of the provided data were chosen for training which required 5000 training epochs to achieve desired. The training is carried out upon the generated data using the Levenberg–Marquardt (LM) algorithm, which is encoded in neural networks toolbox in MATLAB® under 'trainlm' routine.

Neural network is a simplified model of the biological structure found in human brains. This model consists of elementary processing units (also called neurons). It is the large amount of interconnections between these neurons and their capabilities to learn from data to enable neural network as a strong predicting and classification tool. In this study, as mentioned, three-layer feed forward neural network, which con-

sists of an input layer, one hidden layer, and an output layer is selected to predict the responses with MR dampers. The net input value net_k of the neuron k in some layer and the output value O_k of the same neuron can be calculated by the following Eqs. (21)-(22):

$$net_k = \sum w_{jk} O_j \tag{21}$$

$$O_k = f(net_k + \theta_k) \tag{22}$$

where w_{jk} is the weight between the j^{th} neuron in the previous layer and the k^{th} neuron in the current layer, O_j is the output of the j^{th} neuron in the previous layer, $f(.)$ is the neuron's activation function which can be a linear function, a radial basis function, and a sigmoid function, and y_k is the bias of the k^{th} neuron. Feed forward neural network often has one or more hidden layers of sigmoid neurons followed by an output layer of linear neurons. Multiple layers of neurons with nonlinear transfer functions allow the network to learn nonlinear and linear relationships between input and output vectors. In the neural network architecture as shown in Fig. 7, the logarithmic sigmoid transfer function is chosen as the activation function of the hidden layer, Eq. (23):

$$O_k = f(net_k + \theta_k) = \frac{1}{1 + e^{-(net_k + \theta_k)}}. \tag{23}$$

The linear transfer function is chosen as the activation function of the output layer, Eq. (24):

$$O_k = f(net_k + \theta_k) = net_k + \theta_k . \tag{24}$$

We note that neural network needs to be trained before predicting responses. As the inputs are applied to the neural network, the network outputs $(\hat{\cdot})$ are compared with the targets $(.)$. The difference or error between both is processed back through the network to update the weights and biases of the neural network so that the network outputs match closer with the targets. The input and output data are usually represented by vectors called training pairs (f_{k+1}, f_k, $\dot{x}_{k+2}$, $\dot{x}_{k+1}$, $\dot{x}_k$, $\hat{v}_{k+1}$). The process as mentioned above is repeated for all the training pairs in the data set, until the network error converged to a threshold minimum defined by a corresponding performance function. In this research, the Mean Square Error (MSE) function is adopted (desired MSE is 1e-5).

As mentioned, LM algorithm is adapted to train the neural network, which can be written as Eq. (25):

$$w^{i+1} = w^i - \left[\frac{\partial^2 E}{\partial w^{i2}} + \mu I\right]^{-1} \frac{\partial E}{\partial w^i} \tag{25}$$

where i is the iteration index, $\partial E / \partial w^i$ is the gradient descent of the performance function E with respect to the parameter matrix w^i, $\mu \geq 0$ is the learning factor, and I is the unity matrix.

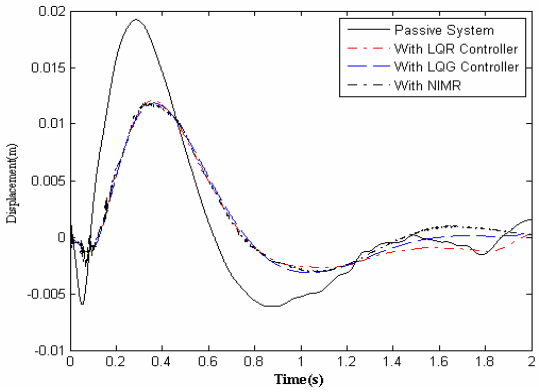

Fig. 9. Displacement of rear-left seat from front left wheel excited with 60km/h.

During the vibration process, the neural network updates the weights and bias of neurons real time in accordance with sampling pairs till the objective error is satisfied, i.e. the property of the system is acquired. As we know, the main aim of the neural network is to predict the desired voltage responses of the system and to provide the desired force of MR dampers. Thus outputs of the neural network are predicted values of voltage $\hat{v}_{k+1}$. In order to accurate prediction, the most direct and important factor which affect the predicted voltage is the feedback of predicted voltage ($\hat{v}_{k+1}$).

7. Results

The full-car model with the MR damper is modeled by the dynamic equations and state space matrices. One of the desired points of this study is to decrease the amplitude of passengers' displacements and sprung mass accelerations, when the suspension system is excited by the road profile. Therefore, the effect of LQR and LQG controllers and the NIMR strategy are simulated for road excitation with calculating their amplitude, and then comparing them with each other. The random road surface is compatibly generated with the power spectral density given in Eq. (20) using a sum of bumpers 7 cm high and 4 cm wide. The displacement and acceleration trajectories for rear-left passenger seat that is excited by the bumper with a height 7 cm and a width 4 cm and with 60 km/h constant velocity in the unpaved road under the front left wheel are shown in Figs. 9 and 10, respectively (Considered system excited by different velocities (e.g. 30, 60 and 75 km/h). Their results, to some extend have the same trend with different amplitude for each velocity. Therefore the results correspond to 60 km/h are shown.). Notice that, in all these graphs, time duration is selected for the best resolution and critical responses happen when the car strikes the bumper.

The graphs show that this system can be controlled as well when the vehicle hits the bumper. The primary oscillations are due to the fewer number of network inputs to train.

On the other hand, there is not a strong history available during the transient state; therefore, the transient part of the

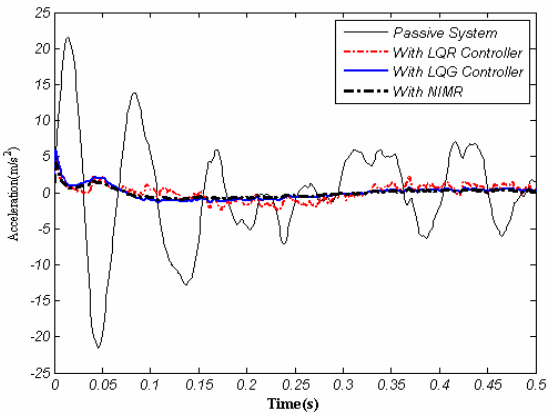

Fig. 10. Acceleration of rear-left seat from front left wheel excited with 60km/h.

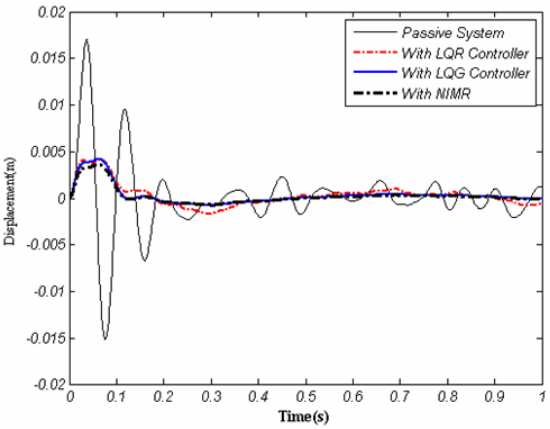

Fig. 11. Road holding for rear-left damper excited with 60 km/h.

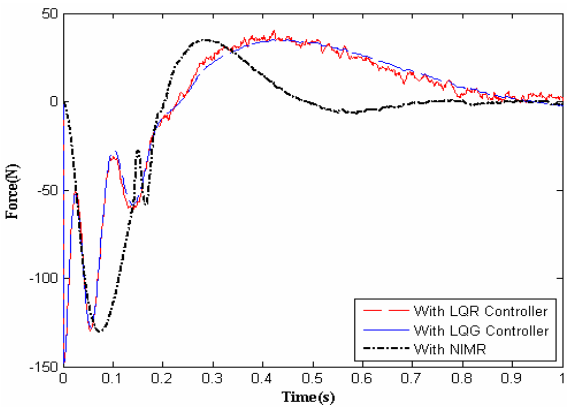

Fig. 12. Generated force by rear-left MR damper from front left wheel excited with 60 km/h.

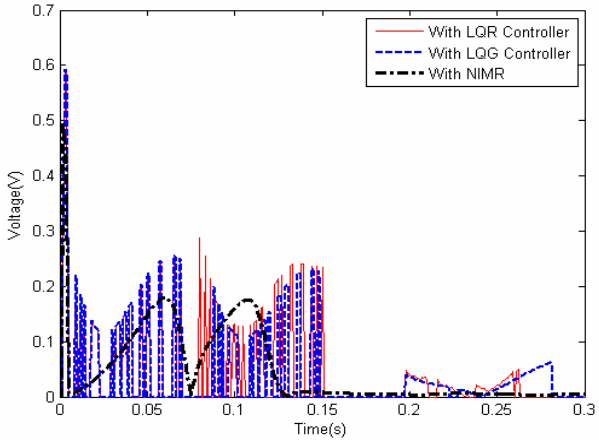

Fig. 13. Requirement voltages to rear-left MR damper from front left wheel excited with 60km/h.

response is not as satisfactory as the steady state part. It is also shown that comfort driving is attained by decreasing (the amplitude of the) acceleration.

The road holding for rear-left damper that is excited by the 7-cm high and 4-cm wide bumper with 60 km/h constant velocity under the front left wheel is shown in Fig. 11.

The stability of the automobile due to using the NIMR strategy is better than the other two strategies because the oscillation of the rear left wheel due to road excitation is less than the others.

The trajectory for the optimal force which produces the desired displacement and acceleration with a velocity of 60 km/h velocity is shown in Fig. 12.

One of the main advantages of NIMR is that control efforts of dampers are less than the LQR and LQG responses, leading to less cost and energy consumption.

The requirement voltage to generate the optimal force is shown in Fig. 13.

According to the graphs above, the trajectories of the NIMR strategy can reduce the amplitude of vibration to some extent similar the optimal controllers with less control effort and oscillation.

8. Conclusions

Usual suspension systems are utilized in vehicles and damp vibration from road profile. However, passive suspension systems have long settling time. When cars are driven in bumpy roads, the passive suspension system driver cannot react effectively. As a result, the usual suspension system cannot damp the excitation with small time intervals. In order to remove this problem the properties of the suspension system should be variable. This task is done by adding MR dampers as actuators to the suspension system.

In order to send commands to the actuator, the LQR controller is utilized. It can decrease the amplitude of the vibration of the passenger seat, but it cannot eliminate the effect of bumpy roads as a disturbance. Therefore, the LQG controller was designed. Unfortunately, due to the inherent nonlinear nature of the MR damper to generate force, a model like that for its inverse dynamics is difficult to mathematically obtain. For this reason, a neural network is constructed to copy the inverse dynamics of the MR damper. According to the graphs above, the trajectories of the NIMR strategy can reduce the amplitude of vibration to some extent similar the optimal con-

trollers with less control effort and oscillations. Therefore, it can increase durability of damper and low cost of production.

Acknowledgment

The authors wish to express their gratitude to the School of Science and Engineering of Sharif University of Technology for supporting this research.

References

[1] S. H. Zareh, A. Sarrafan, A. A. A. Khayyat and A. Zabihollah, Intelligent semi-active vibration control of eleven degrees of freedom suspension system using magnetorheological dampers, *Journal of Mechanical Science and Technology*, 26 (2) (2012) 323-334.

[2] S. H. Zareh and A. A. A. Khayyat, Fuzzy inverse model of magnetorheological dampers for semi-active vibration control of an eleven-degrees of freedom suspension system, *Journal of System Design and Dynamics*, 5 (7) (2011) 1485-1497.

[3] R. S. Prabakar, C. Sujatha and S. Narayanan, Optimal semi-active preview control response of a half car vehicle model with magnetorheological damper, *Journal of sound and vibration,* 326 (2009) 400-420.

[4] M. S. Yahaya and H. S. Johari, Modeling and control of the active suspension system using proportional integral sliding mode approach, *Asian Journal of Control,* 7 (2) (2005) 91-98.

[5] S. H. Zareh, A. Sarrafan and A. A. A. Khayyat, Clipped optimal control of 11-DOFs of a passenger car using magnetorheological damper, *International Conference on Computer Control and Automation* (2011) 162-167.

[6] M. M. M. Salem and A. A. Ayman, Fuzzy control of a quarter-car suspension system, *World Academy of Science Engineering and Technology*, 53 (2009) 258-263.

[7] H. C. Sohn and K. T. Hong, An adaptive LQG control for semi-active suspension systems, *International Journal Vehicle Design,* 34 (4) (2004) 309-326.

[8] M. Biglarbegian, W. Melek and F. Golnaraghi, Intelligent control of vehicle semi-active suspension system for improved ride comfort and road handling, *Fuzzy Information Processing Society* (2006) 19-24.

[9] O. Yoshida and S. J. Dyke, Seismic control of a nonlinear benchmark building using smart dampers, *Journal of engineering mechanics,* 130 (2004) 386-392.

[10] Y. Kim, R. Langari and S. Hurlebaus, Semi-active nonlinear control of a building with a magnetorhelogical damper system, *Mechanical Systems and Signal Processing,* 23 (2009) 300-315.

[11] M. Ahmadian and C. A. Pare, A quarter car experimental analysis of alternative semi-active control methods, *Journal of Intelligent Material Systems and Structures,* 11 (8) (2000) 604-612.

[12] J. S. Chiou and T. M. Liu, Using fuzzy logic controller and evolutionary genetic algorithm for automotive active suspension system, *International Journal of Automotive Technology*, 10 (6) (2009) 703-710.

[13] J. Sun and Q. Yang, Modeling and intelligent control of vehicle active suspension system, *IEEE International conference on RAM* (2008) 239-242.

[14] S. Yildirim and I. Eski, Vibration analysis of an experimental suspension system using artificial neural networks, *Journal of Scientific & Industrial Research,* 68 (2009) 522-529.

[15] V. S. Atray and P. N. Roschke, Neuro-fuzzy control of railcar vibrations using semi active dampers, *Computer-Aided Civil and Infrastructure Engineering,* 19 (2004) 81-92.

[16] S. H. Sadati, M. A. Shooredeli and A. D. Panah, Designing a neuro-fuzzy controller for a vehicle suspension system using feedback error learning, *Journal of mechanics and aerospace*, 4 (3) (2008) 45-57.

[17] M. T. Hagan and M. B. Menhaj, Training feedforward networks with the Marquardt algorithm, *IEEE Trans. on Neural Networks*, 5 (6) (1994) 989-993.

[18] A. Khajekaramodin and H. Haji-Kazemi, A. Rowhanimanesh and M. R. Akbarzadeh, Semi-active control of structures using neuro-inverse model of MR dampers, *Proc. of First Joint Congress on Fuzzy and Intelligent Systems*, Mashhad, Iran (2007) 789-803.

[19] A. Sarrafan, S. H. Zareh, A. A. A. Khayyat and A. Zabihollah, Neuro-fuzzy control strategy for an offshore steel jacket platform subjected to wave-induced forces using magnetorheological dampers, *Journal of Mechanical Science and Technology*, 26 (4) (2012) 1-18.

[20] Y. W. Yun, S. M. Lee and M. Park, A study on the efficiency improvement of a passive oil damper using an MR accumulator, *Journal of Mechanical Science and Technology*, 24 (11) (2010) 2297-2305.

[21] Z. D. Xu and Y. Q. Guo, Neuro-fuzzy control strategy for earthquake-excited nonlinear magnetorheological structures, *Soil Dynamics and Earthquake Engineering*, 28 (2008) 717-727.

Seiyed Hamid Zareh was born in 1983 and received his B.Sc. degree from the Technical Faculty of Imam Hossein University, Tehran, Iran, in 2006 and his M.Sc. degree from School of Science and Engineering of Sharif University of Technology, Iran, in 2011, all in mechanical and mechatronics engineering. This author became a member of IEEE in 2011. His research interests are mechatronics system, smart materials and structures, automatic control, and intelligent control. He has one book in the field of oil and gas with the title of "Storage Tank Design", (2005) and one book chapter (2011). He also published four journal and twelve international conference papers. Mr. Zareh is also a member of American Society of Mechanical Engineers (ASME) and Iranian Society of Mechanical Engineers (ISME). He received oral presentation awards at the 2nd, 3rd and 4th symposium in research week in 2009, 2010, 2011 and technical presentation in Singapore 2009, respectively.